

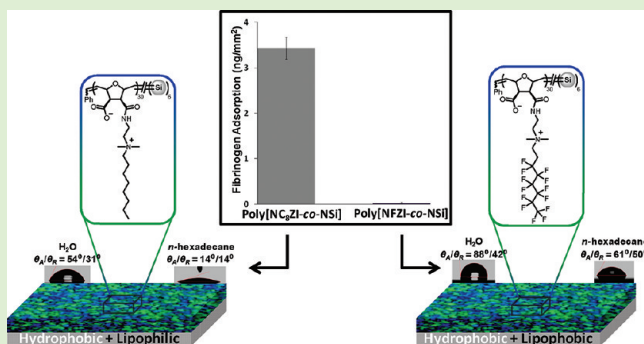
# Amphiphilic Polybetaines: The Effect of Side-Chain Hydrophobicity on Protein Adsorption

Semra Colak and Gregory N. Tew\*

Department of Polymer Science and Engineering, University of Massachusetts – Amherst, Conte Research Center for Polymers, 120 Governor's Drive, Amherst, Massachusetts 01003, United States

## Supporting Information

**ABSTRACT:** Novel amphiphilic polybetaines were synthesized and used as the base material for nonfouling coatings. The amphiphilicity of these polybetaines was systematically tuned by coupling chains of increasing hydrophobicity to the zwitterionic functionality side at the repeat unit level. An oligoethylene glycol (OEG) moiety was selected to yield the most hydrophilic coating, while octyl (C<sub>8</sub>) and fluorinated (F) groups were used to impart lipophilicity and lipophobicity to the coatings, respectively. This unique design allowed us to investigate the effect of the lipophilicity/lipophobicity of the side chain on the nonfouling properties of these zwitterionic systems. Adsorption studies, performed using six different proteins, showed that the fluorinated polybetaine, Poly[NFZI-co-NSi], resisted nonspecific adsorption as effectively as, and in some cases even better than, the most hydrophilic Poly[NOEGZI-co-NSi] coating. The comparison of Poly[NFZI-co-NSi] to its noncharged analog demonstrated the essential nature of the zwitterionic functionality in imparting nonfouling character to the coating.



## INTRODUCTION

A unique series of amphiphilic betaine copolymers, designed to explore the effect of increasing the hydrophobicity on the nonfouling properties of surfaces, is introduced. Fouling studies showed that a zwitterionic surface with both hydrophobic and lipophobic properties resists protein adsorption as well as one with only hydrophilic character. Biofilm formation on substrates, caused by the attachment and growth of microorganisms in aqueous environments, is a ubiquitous problem that can lead to various adverse events.<sup>1</sup> These include, but are not limited to, thrombosis, microbial infections, and reduction in the efficacy/sensitivity of devices.<sup>2</sup> A key challenge in preventing biofilm formation is the design of smart materials or engineered surfaces that can effectively resist the irreversible attachment of a wide variety of species including proteins, microbial cells, and spores.<sup>2–5</sup> Among many approaches investigated, hydrophilic modification of surfaces using poly(ethylene glycol) (PEG),<sup>4,6–8</sup> and more recently, zwitterionic polymers<sup>5,9–11</sup> with high wettability were found to be among the most promising candidates. However, larger microorganisms as well as proteins are inherently amphiphilic. They operate by different attachment mechanisms, with some having higher affinity to hydrophobic surfaces and others to hydrophilic.<sup>12,13</sup> Therefore, solely hydrophilic or hydrophobic surfaces are often inadequate in resisting fouling upon prolonged exposure to complex environments such as blood.<sup>14</sup> With these findings, there is increasing awareness for engineering amphiphilic materials, which, similar to living

organisms, can restructure their surfaces depending on the environment.<sup>15,16</sup>

The first example of an amphiphilic nonfouling material was reported by Wooley and coworkers, where hyperbranched fluoropolymers (HBFPs) were cross-linked with linear PEG chains to obtain coatings with complex surface morphologies.<sup>17,18</sup> Because of the incompatibility of the hydrophilic and hydrophobic domains, these coatings showed phase segregation, resulting in topological surface roughness when immersed in aqueous media. The nonfouling performance of these cross-linked, amphiphilic networks was tested using various biomacromolecules with adhesion affinity to either hydrophilic or hydrophobic substrates.<sup>19</sup> The results showed that independent of the adhesion preference of proteins and the larger microorganisms tested, the amphiphilic coatings, HBFP-PEG, were more effective in resisting nonspecific adsorption than the coatings composed of only HBFP or PEG. In a similar example, a surface-active block copolymer (SABC) was developed and used to prepare antifouling coatings by Ober and coworkers.<sup>15,20–24</sup> The SABC was composed of a polystyrene block and a comb-like amphiphilic block, in which both PEG and fluoroalkyl groups were on the same side chain. The effectiveness of these coatings was tested for resistance to bovine serum albumin<sup>25</sup> (BSA) and marine algae

Received: January 4, 2012

Revised: March 26, 2012

Published: April 19, 2012

adsorption.<sup>20</sup> When compared to the controls [poly(dimethylsiloxane) and the base coat of SABCs: poly(styrene-*b*-ethylene butylene-*b*-styrene)], the surfaces composed of the SABCs showed lower BSA adsorption. More recently, amphiphilic self-assembled monolayers (SAMs), likewise composed of fluoroalkyl and PEG groups, were also reported as potential nonfouling surfaces.<sup>26–28</sup> The protein adsorption studies of these SAMs yielded similar results, where the amphiphilic systems were more effective in resisting nonspecific protein adsorption than only PEG or fluoroalkyl SAMs.

These examples show that besides wettability, compositional and morphological heterogeneities are also critical parameters for designing effective nonfouling materials. Although there are several examples of amphiphilic materials obtained by incorporation of either hydrocarbon or fluorine-based hydrophobic moieties, no direct comparison between both has been reported.<sup>29,30</sup> Moreover, all of these systems employ PEG as the hydrophilic component, which is known to be unstable in the presence of oxygen and transition metals, reducing the lifetime of the material.<sup>31</sup> Therefore, the quest to identify the most effective components that yield optimal amphiphilic systems is still ongoing.

In this Communication, we introduce a series of novel amphiphilic polybetaine copolymers composed of zwitterionic functionalities coupled with hydrophilic/hydrophobic alkyl side chains within the same repeat unit (Figure 1). This unique

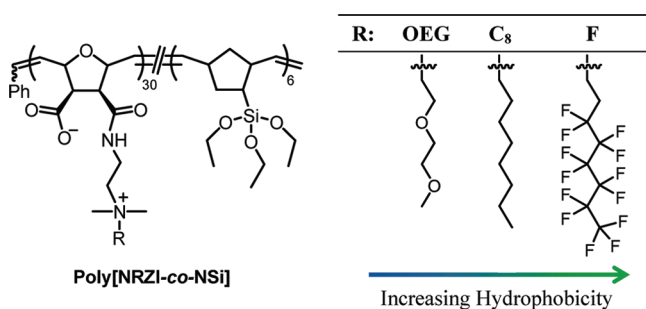


**Figure 1.** Summary of copolymers synthesized. Nomenclature: R = substituent, N = norbornene, ZI = zwitterion, Si = 5-bicycloheptenyl triethoxysilane repeat unit, OEG = oligoethylene glycol, C<sub>8</sub> = octyl, and F = 1H,1H,2H,2H-perfluorooctyl.

design allowed us to systematically tune the amphiphilicity of the whole system at the repeat unit level. In this system, a betaine was employed as the hydrophilic component, and the substituent (R) was varied as oligoethylene glycol (OEG), octyl (C<sub>8</sub>), and fluorinated (F) chains to systematically tune the overall amphiphilicity. All polymers were synthesized as silane-containing copolymers via ring-opening metathesis polymerization (ROMP), where an ethoxysilane-containing monomer

was used as the minor component.<sup>32</sup> A ratio of 15–20 mol % was used, sufficient to provide covalent attachments to the substrate (glass/silica surface) as well as to improve the stability of the coatings through interchain cross-linking.<sup>33,34</sup>

## ■ RESULT AND DISCUSSION

To prevent the carboxylate anion of the zwitterion from retarding the ROMP kinetics,<sup>35,36</sup> the monomers were synthesized as cationic precursors through the quaternization of a norbornene-based tertiary amine (Scheme S1 and Figures S1–S6 in the Supporting Information). The resulting quaternary ammonium precursor monomers were then copolymerized in a random fashion with 5-bicycloheptenyl triethoxysilane (Scheme S3 in the Supporting Information) via ROMP. The monomer compositions and the molecular weights of the resulting copolymers were determined using <sup>1</sup>H NMR end-group analysis and were in strong agreement with the theoretical values, indicating successful polymerization. Detailed synthetic procedures as well as molecular weight characterization of the copolymers can be found in the Supporting Information (Figures S7–S12, Table S1). Surfaces were prepared via spin coating a 1% w/v trifluoroethanol solution of each polymer on a freshly cleaned silica wafer. These surfaces were then dried under vacuum to remove the remaining solvent, subjected to hydrolysis, and cured above the condensation temperature of the ethoxysilane units. The resulting cationic coatings (Poly[NR(+)-co-NSi]) were then postfunctionalized using dilute base (0.1 M NaOH) to obtain their corresponding zwitterionic counterparts (Poly[NRZI-co-NSi]).<sup>32,35</sup> Detailed surface characterization of the ring-opening transformation of Poly[NF(+)-co-NSi] can be found in the Supporting Information (Figure S13), while the data for Poly[NOEG(+)-co-NSi] and Poly[NC<sub>8</sub>(+)-co-NSi] were reported elsewhere.<sup>32</sup> Coating thicknesses were measured using single-wave ellipsometry and were in the range of 20 to 35 nm.

The performance of a coating is strongly dependent on its surface properties, such as wettability, morphology, and interfacial characteristics. Therefore, prior to protein adsorption studies, detailed surface characterization was performed on the coatings. The wettability of the zwitterionic coatings, Poly[NRZI-co-NSi], was analyzed via contact angle (CA) measurements using the sessile drop technique. Advancing and receding CAs were measured with water and *n*-hexadecane. While water was used to determine the relative hydrophilicity/hydrophobicity of the coatings, *n*-hexadecane was employed to determine their lipophilicity/lipophobicity. The results are summarized in Table 1. (Surface characterization results of the cationic precursor coatings can be found in the Supporting Information Table S2.) Independent of the probing liquid used,

**Table 1.** Roughness, Contact Angle, and Surface Free Energy Measurements of the Zwitterionic Coatings

polymer	R <sub>t</sub> (min) <sup>b</sup>	roughness (nm) <sup>c</sup>	water CA (°) <sup>a</sup>			<i>n</i> -hexadecane CA (°)			surface free energy (mN/m)		
			θ <sub>W-S</sub>	θ <sub>W-A</sub>	θ <sub>W-R</sub>	θ <sub>H-S</sub>	θ <sub>H-A</sub>	θ <sub>H-R</sub>	γ <sub>S</sub> <sup>d</sup>	γ <sub>S</sub> <sup>p</sup>	γ <sub>S</sub>
poly[NOEGZI-co-NSi]	5.9	0.52	32 ± 1	32 ± 2	18 ± 1	2 ± 0	14 ± 1	2 ± 0	26.8	36.4	63.2
poly[NC <sub>8</sub> ZI-co-NSi]	30.9	1.32	70 ± 3	54 ± 1	31 ± 1	2 ± 0	14 ± 1	15 ± 2	26.8	22.2	49.0
poly[NFZI-co-NSi]	40.7	9.11	89 ± 1	88 ± 3	42 ± 4	62 ± 2	61 ± 2	50 ± 1	15.2	7.4	22.6

<sup>a</sup>Contact angle (CA), θ<sub>W-S</sub> (static water CA), θ<sub>W-A</sub> (advancing water CA), and θ<sub>W-R</sub> (receding water CA) <sup>b</sup>Retention time (R<sub>t</sub>) of the corresponding monomers as measured by HPLC using a C<sub>8</sub> column with a gradient of 1% CH<sub>3</sub>CN/min starting with 100% water. <sup>c</sup>Measured using tapping mode atomic force microscopy (AFM) on the dry coating.

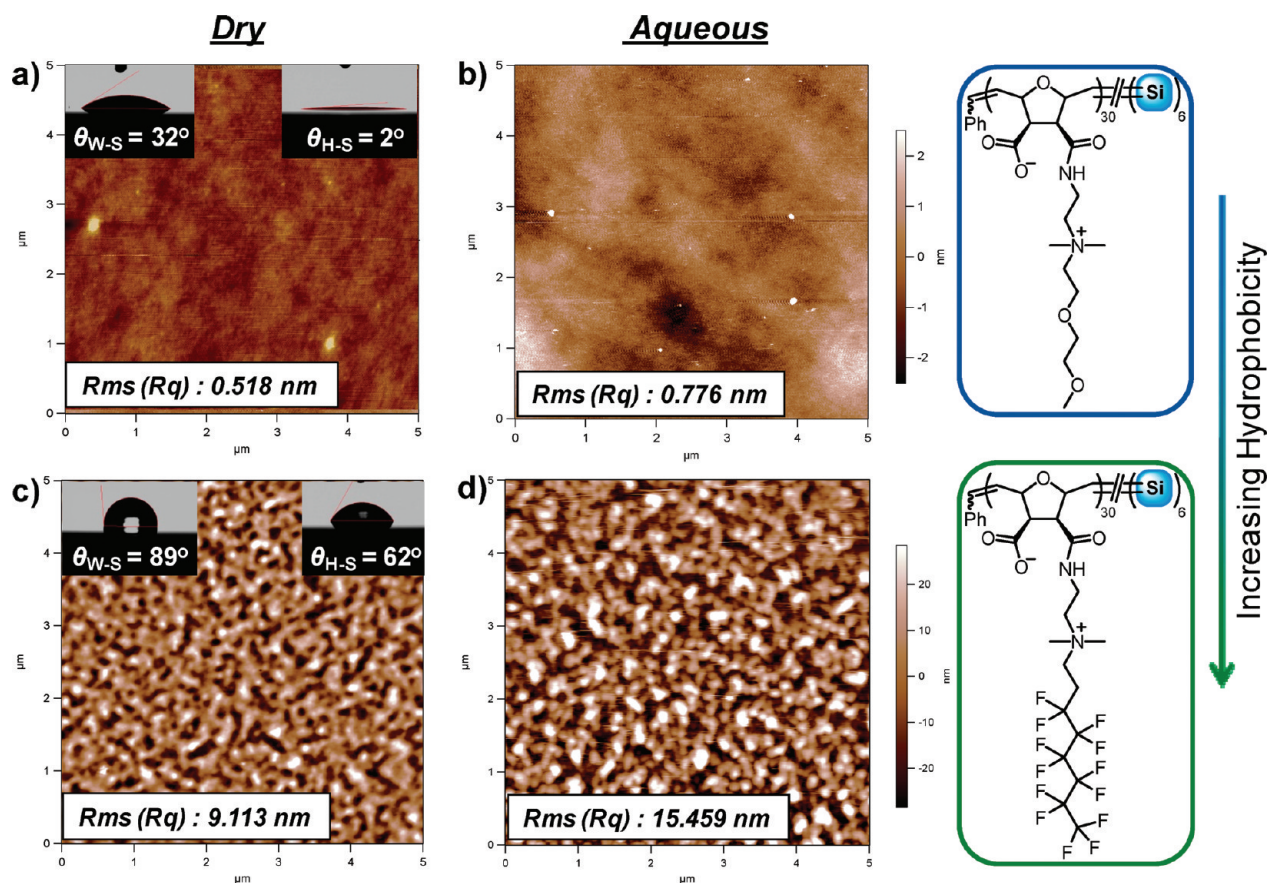


**Figure 2.** AFM surface roughness analysis of Poly[NOEGZI-co-NSi] (a) dry coating in air and (b) hydrated coating in PBS for 24 h. Surface roughness analysis of Poly[NFZI-co-NSi] (c) dry coating in air and (d) hydrated coating in PBS for 24 h. Insets in panels a and c show the static contact angle analyses of the corresponding surfaces using (left) water and (right) *n*-hexadecane.

the general trend observed for the zwitterionic coatings was that their wetting was strongly influenced by the polarity of their side chains. The most hydrophilic coating was Poly[NOEGZI-co-NSi] with  $\theta_{W-A}/\theta_{W-R} = 32^\circ/18^\circ$  for water. Both Poly[NC<sub>8</sub>ZI-co-NSi] ( $\theta_{W-A}/\theta_{W-R} = 54^\circ/31^\circ$ ) and Poly[NFZI-co-NSi] ( $\theta_{W-A}/\theta_{W-R} = 88^\circ/42^\circ$ ) were more hydrophobic than Poly[NOEGZI-co-NSi], with Poly[NFZI-co-NSi] being the most hydrophobic. These results were in agreement with the retention times ( $R_t$ ) of the corresponding zwitterionic monomers, as measured by HPLC (Table 1). One important difference between Poly[NC<sub>8</sub>ZI-co-NSi] and Poly[NFZI-co-NSi] was their wetting behavior with *n*-hexadecane. While Poly[NC<sub>8</sub>ZI-co-NSi] showed lower CA values,  $\theta_{H-A}/\theta_{H-R} = 14^\circ/15^\circ$ , indicating strong interaction with the nonpolar liquid, Poly[NFZI-co-NSi] ( $\theta_{H-A}/\theta_{H-R} = 61^\circ/50^\circ$ ) kept a high CA. This result indicates that while Poly[NFZI-co-NSi] possesses an overall lipophobic character Poly[NC<sub>8</sub>ZI-co-NSi] is lipophilic. It is important to note this difference as the effect of the lipophilicity/lipophobicity of these amphiphilic betaines on their nonfouling performance is investigated here.

All of the coatings demonstrated hysteresis ( $\Delta\theta = \theta_A - \theta_R$ ) in water upon dynamic CA analysis, and the largest value was obtained for Poly[NFZI-co-NSi] ( $\Delta\theta_W = 46^\circ \pm 1^\circ$ ). In general, CA hysteresis can be attributed to several factors, including surface roughness, swelling of the coating, and surface restructuring or mobility.<sup>37</sup> Since all of these parameters may also influence the nonfouling properties of the coatings,<sup>19</sup> the possible reasons leading to the observed hysteresis were investigated further. Tapping mode atomic force microscopy

(AFM) on the dry coatings was done to obtain their roughness profiles. Poly[NOEGZI-co-NSi] and Poly[NC<sub>8</sub>ZI-co-NSi] yielded relatively smooth surfaces (Table 1), whereas Poly[NFZI-co-NSi] had the highest surface roughness (9.1 nm) (Figure 2a,c). A plausible explanation for the high surface roughness of Poly[NFZI-co-NSi] is the increased incompatibility of the amphiphilic system, arising from the incorporation of a fluorinated tail to a hydrophilic betaine. Similarly, Poly[NC<sub>8</sub>ZI-co-NSi], which is more hydrophobic than Poly[NOEGZI-co-NSi], also showed higher roughness (1.3 nm). However, when compared to previously published reports,<sup>38–40</sup> the roughness values of these coatings are still quite small and likely not large enough to be the sole reason of hysteresis. Therefore, other possible factors, such as swelling of the coatings as well as the reorientation/mobility of the polymer side chains, were investigated via more detailed surface characterization studies, including AFM under aqueous environment and X-ray diffraction.

Tapping mode AFM in an aqueous solution of the hydrated coatings (immersed in phosphate-buffered saline (PBS)) was done on the same equipment used to obtain the dry images to avoid any instrumental differences. The analysis was performed on Poly[NOEGZI-co-NSi] and Poly[NFZI-co-NSi] as these were the most hydrophilic and hydrophobic coatings, respectively. The images of the dry and hydrated coatings are shown in Figure 2a–d. Upon hydration, both coatings showed an increase in their relative roughness due to swelling of their hydrophilic domains; however, their overall morphology remained the same. The Poly[NFZI-co-NSi] showed a larger

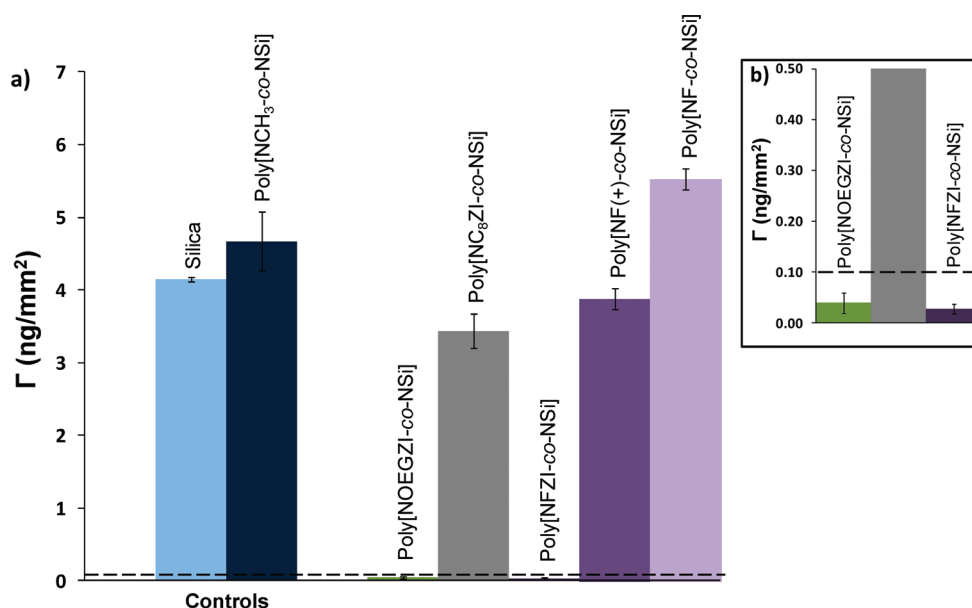


**Figure 3.** (a) Fibrinogen adsorption on various surfaces. Dotted line indicates 0.1 ng/mm<sup>2</sup> protein adsorption limit that can induce full-scale biofilm formation, resulting in the loss of function of the implantable device.<sup>58</sup> The inset (b) is the expanded version of the y axis showing the protein adsorption amounts on Poly[NOEGZI-co-NSi] and Poly[NFZI-co-NSi] with respect to the dotted line. Error bars represent standard error obtained from three independent measurements.

increase in roughness, in accordance with its hysteresis characteristics. Among all coatings, Poly[NFZI-co-NSi] had the highest water CA hysteresis ( $\Delta\theta_W = 46^\circ \pm 1^\circ$ ), indicating strong surface rearrangement in polar media, whereas this value was much lower for the nonpolar *n*-hexadecane ( $\Delta\theta_H = 11^\circ \pm 1^\circ$ ).

To investigate the surface conformation of the fluorinated alkyl side chains, we performed powder X-ray diffraction (XRD)<sup>40–43</sup> (Figure S14 of the Supporting Information). The spectrum revealed no sharp peaks indicative of oriented side chains; only a broad diffusion band at 5.1 Å, characteristic of an amorphous state, was observed. These results were consistent with the literature where it has been suggested that more than eight perfluorinated carbons per side chain are needed to yield an ordered conformation on the surface.<sup>40–43</sup> In fact, it has been shown that polymers composed of chains with less than six fluorinated carbons remain amorphous. These materials are generally characterized by their poor dynamic water repellency due to high surface mobility, which is more predominantly observed for systems containing polar components.<sup>40,43</sup> These conclusions are consistent with our observations, where Poly[NFZI-co-NSi] showed amorphous morphology of its fluorinated side chains by XRD analysis and high hysteresis in polar media ( $\Delta\theta_W = 46^\circ \pm 1^\circ$ ) by dynamic CA analysis. Both of these results indicate high surface mobility due to environmentally dependent chain reorganization of Poly[NFZI-co-NSi].

To further investigate and distinguish the contribution of different interaction components at the solid–liquid interface, such as van der Waals dispersive, dipole, and hydrogen bonding, we determined surface free energies of the coatings according to the Owens, Wendt, and Kaelble method.<sup>19,44,45</sup> Even though this is a widely accepted method to calculate surface free energies of solid materials, it is solely dependent on CA values, which may be affected by chain rearrangement or roughness on the surface.<sup>19,46</sup> To eliminate such effects and have more accurate calculations, we used the advancing CA

values, which are believed to be the least affected by surface heterogeneities.<sup>19,47</sup> The total surface energies ( $\gamma_S = \gamma_S^p + \gamma_S^d$ ), the polar ( $\gamma_S^p$ ), and the dispersive ( $\gamma_S^d$ ) components obtained for the coatings are summarized in Table 1. The highest surface free energy was observed for Poly[NOEGZI-co-NSi] ( $\gamma_S = 63.2$  mN/m), in which both the dispersive and polar components contributed significantly, as expected. Even though Poly[NOEGZI-co-NSi] and Poly[NC<sub>8</sub>ZI-co-NSi] had the same value for their dispersive components ( $\gamma_S^d = 26.8$  mN/m), their polar components were significantly different. Poly[NOEGZI-co-NSi] had higher polar character than Poly[NC<sub>8</sub>ZI-co-NSi] due to the ability of the OEG side chains to form hydrogen bonds with the surrounding water molecules. Not surprisingly, Poly[NFZI-co-NSi] had the lowest surface energy ( $\gamma_S = 22.6$  mN/m), indicating high surface coverage of the fluorinated side chains, yielding the lipophobic character. It is important to note that although Poly[NFZI-co-NSi] contains zwitterionic functionalities, its surface energy is similar to the surface energy of polytetrafluoroethylene (PTFE) ( $\gamma_S \approx 18$  mN/m), a fluorinated material commonly used in biomedical applications.<sup>40,48–50</sup>

Protein adsorption on all non-natural surfaces results from a combination of weak electrostatic and hydrophobic interactions.<sup>26</sup> Therefore, our main design criteria of these materials was to effectively eliminate such interactions. The resistance to protein adsorption of the resulting coatings was evaluated using six different proteins. To make direct comparisons to the previous literature reports, the most commonly studied proteins were employed: BSA, fibrinogen, and lysozyme.<sup>32</sup> However, these proteins have different molecular weights, which has been shown to affect their adsorption mechanism.<sup>32,51,52</sup> Therefore, in addition, myoglobin, cytochrome *c*, and succinic anhydride-modified lysozyme were used as proteins having similar molecular weights but different isoelectric points under physiological conditions.<sup>32</sup> Ellipsometry measurements<sup>53–55</sup> were done to quantify the amount of adsorbed protein, and fluorescence microscopy<sup>56,57</sup> was employed for qualitative analysis, using fluorescein isothiocya-

Table 2. Protein Adsorption on the Coatings As Measured by Ellipsometry Measurements

polymer	protein adsorption amount (ng/mm <sup>2</sup> )					
	BSA	fibrinogen	lysozyme	SA-lysozyme	myoglobin	cytochrome <i>c</i>
poly[NOEGZI- <i>co</i> -NSi]	0.05 ± 0.01	0.04 ± 0.02	0.65 ± 0.11	0.26 ± 0.02	0.24 ± 0.06	0.41 ± 0.08
poly[NOEG(+)- <i>co</i> -NSi]	10.4 ± 0.27	1.90 ± 0.15	1.65 ± 0.36	2.44 ± 0.02	4.30 ± 0.12	1.19 ± 0.08
poly[NC <sub>8</sub> ZI- <i>co</i> -NSi]	4.79 ± 1.04	3.44 ± 0.24	3.51 ± 0.58	1.95 ± 0.22	1.63 ± 0.10	1.30 ± 0.04
poly[NC <sub>8</sub> (+)- <i>co</i> -NSi]	6.54 ± 0.84	10.6 ± 0.44	3.54 ± 0.10	11.2 ± 0.01	6.04 ± 0.03	3.18 ± 0.14
poly[NFZI- <i>co</i> -NSi]	0.08 ± 0.02	0.03 ± 0.01	0.14 ± 0.11	0.25 ± 0.05	0.30 ± 0.06	0.84 ± 0.20
poly[NF(+)- <i>co</i> -NSi]	2.81 ± 0.39	3.88 ± 0.15	2.35 ± 0.66	2.11 ± 0.39	0.94 ± 0.04	0.89 ± 0.31
poly[NF- <i>co</i> -NSi]	1.98 ± 0.14	5.52 ± 0.15	1.71 ± 0.02	1.36 ± 0.20	1.75 ± 0.08	1.92 ± 0.02
poly[NCH <sub>3</sub> - <i>co</i> -NSi]	1.07 ± 0.09	4.67 ± 0.40	2.94 ± 0.16	1.70 ± 0.04	1.04 ± 0.10	2.62 ± 0.11
silica	0.47 ± 0.10	4.15 ± 0.02	1.29 ± 0.10	0.49 ± 0.10	1.37 ± 0.03	2.02 ± 0.10

nate (FITC)-labeled BSA to visually study the protein adsorption.<sup>32</sup> Figure 3 shows fibrinogen adsorption on the amphiphilic polybetaines in comparison with control surfaces, including clean silica and a neutral hydrophobic control, Poly[NCH<sub>3</sub>-*co*-NSi], as well as the cationic precursor, Poly[NF(+)-*co*-NSi], and the noncharged fluoropolymer, Poly[NF-*co*-NSi] (Supporting Information, Scheme S3). The summary of all protein adsorption results of the zwitterionic coatings and their cationic precursors, including fluorescence microscopy images, can be found in Table 2 and the Supporting Information (Figures S15–17).

Independent of the protein used, both Poly[NOEGZI-*co*-NSi] and Poly[NFZI-*co*-NSi] were effective in resisting protein adsorption, whereas Poly[NC<sub>8</sub>ZI-*co*-NSi] consistently showed higher adsorption (Table 2 and Figure S15 of the Supporting Information). As shown in Figure 3, the fibrinogen adsorption on both Poly[NOEGZI-*co*-NSi] ( $\Gamma_{\text{FIB}} = 0.039 \pm 0.02$  ng/mm<sup>2</sup>) and Poly[NFZI-*co*-NSi] ( $\Gamma_{\text{FIB}} = 0.027 \pm 0.01$  ng/mm<sup>2</sup>) was lower than the 0.1 ng/mm<sup>2</sup> limit, which is the amount of fibrinogen adsorbed on a surface that can induce full scale biofilm formation, resulting in the loss of function of the implantable device.<sup>46</sup> While the ability of Poly[NOEGZI-*co*-NSi] toward resisting protein adsorption was expected due to its hydrophilicity, given the hydrophobic nature of Poly[NFZI-*co*-NSi], its performance was surprising. We and others have previously shown that within a given system, as the hydrophobicity of the coating increases, its ability to resist nonspecific adsorption decreases.<sup>32,59</sup> However, in the case of Poly[NFZI-*co*-NSi], which had the highest hydrophobicity among all of the coatings investigated, it is clear that its ability to resist protein adsorption is due to the presence of fluorinated side chains. This can be better seen when the protein adsorption of Poly[NFZI-*co*-NSi] is compared with Poly[NC<sub>8</sub>ZI-*co*-NSi] (Figure S15 of the Supporting Information). Although both coatings are strongly hydrophobic, Poly[NFZI-*co*-NSi] possess a lipophobic character, resulting in a repulsive effect against both polar and nonpolar (lipophilic) components of the protein. The direct comparison between the resistance of Poly[NC<sub>8</sub>ZI-*co*-NSi] and Poly[NFZI-*co*-NSi] to protein adsorption demonstrates the importance of employing lipophobic moieties rather than lipophilic ones as the hydrophobic component in amphiphilic systems for nonfouling applications.

Since perfluorinated substances are known to be chemically inert to both hydrophilic and lipophilic media,<sup>60–62</sup> it is important to distinguish what role the zwitterionic functionality is playing in this system. With that aim, Poly[NF-*co*-NSi], a noncharged analog of Poly[NFZI-*co*-NSi], was synthesized. (See the Supporting Information for the detailed synthetic procedure.) The surface properties and the nonfouling

character of Poly[NFZI-*co*-NSi] were investigated in comparison with Poly[NF-*co*-NSi] as well as its cationic precursor, Poly[NF(+)-*co*-NSi]. Figure S16 of the Supporting Information shows the surface properties of all three fluorinated systems, including surface roughness, wetting properties, and adsorption of FITC-BSA. All coatings showed relatively high hydrophobicities with water CAs greater than  $\theta_A = 85^\circ$  as well as very similar surface roughness values ranging from 4.6 (for Poly[NF-*co*-NSi]) to 10.2 nm (for Poly[NFZI-*co*-NSi]). The most significant difference observed among these coatings was their resistance to FITC-BSA adsorption. Poly[NFZI-*co*-NSi] outperformed both the noncharged and the cationic counterparts. Also, shown in Figure 3, both Poly[NF(+)-*co*-NSi] ( $\Gamma_{\text{FIB}} = 3.88 \pm 0.15$  ng/mm<sup>2</sup>) and Poly[NF-*co*-NSi] ( $\Gamma_{\text{FIB}} = 5.5 \pm 0.15$  ng/mm<sup>2</sup>) showed higher fibrinogen adsorption than Poly[NFZI-*co*-NSi] ( $\Gamma_{\text{FIB}} = 0.027 \pm 0.01$  ng/mm<sup>2</sup>). This observation was consistent for all different proteins investigated. (See Table 2 and Figure S17 of the Supporting Information.) While all of these fluorinated coatings had similar surface characteristics (roughness and wetting properties), they were composed of different overall charges. In comparison with the zwitterionic Poly[NFZI-*co*-NSi], the cationic Poly[NF(+)-*co*-NSi] showed high protein adsorption, apparently dominated by the electrostatic attractions. This observation demonstrates the importance of screening the electrostatic interactions in addition to the lipophilic ones. Moreover, the superior performance of Poly[NFZI-*co*-NSi] ( $\Gamma_{\text{FIB}} = 0.027 \pm 0.01$  ng/mm<sup>2</sup>,  $\gamma_S = 22.6$  mN/m) over the noncharged analog, Poly[NF-*co*-NSi] ( $\Gamma_{\text{FIB}} = 5.5 \pm 0.15$  ng/mm<sup>2</sup>,  $\gamma_S = 12.8$  mN/m), demonstrates the importance of the zwitterionic functionality in the system. The amount of protein adsorption observed on Poly[NF-*co*-NSi] was similar to the values previously reported for PTFE ( $\Gamma_{\text{FIB}} \approx 1.5$  ng/mm<sup>2</sup>–5.5 ng/mm<sup>2</sup>,  $\gamma_S \approx 18$  mN/m).<sup>40,49,50</sup>

One plausible explanation to the efficacy of Poly[NFZI-*co*-NSi] in resisting nonspecific protein adsorption as effectively as Poly[NOEGZI-*co*-NSi] is the increased surface coverage of the zwitterionic functionality, which is aided by the low surface energy of the fluorinated side chains. While this is not directly evident from the wetting experiments performed on Poly[NFZI-*co*-NSi], both the high hysteresis of the surface as well as the amorphous morphology observed from XRD analysis indicate fast surface rearrangement. Although the high water CA of Poly[NFZI-*co*-NSi] is indicative of a large concentration of fluorinated side chains on the surface, they can reorganize when immersed in hydrophilic media to expose the zwitterionic functionalities on the surface. This results in a surface with high surface coverage of zwitterionic units. The effectiveness of the fluorinated side chains in increasing the zwitterionic surface

coverage becomes more evident when Poly[NFZI-co-NSi] is compared with Poly[NC<sub>8</sub>ZI-co-NSi]. Even though Poly[NC<sub>8</sub>ZI-co-NSi] is more hydrophilic ( $\theta_{W-A}/\theta_{W-R} = 54^\circ/31^\circ$ ) than Poly[NFZI-co-NSi] ( $\theta_{W-A}/\theta_{W-R} = 89^\circ/62^\circ$ ) it shows higher protein adsorption. These observations are consistent with previously published reports, where detailed surface characterization demonstrated the effectiveness of using low-surface energy fluorinated units to improve the surface coverage of amphiphilic systems (PEG was used as the hydrophilic component).<sup>15,22,25,26</sup>

## CONCLUSIONS

We have designed a series of novel zwitterion-based, amphiphilic coatings for nonfouling applications. The hydrophobicity of the system was tuned by the incorporation of side chains to the unique zwitterionic functionality at a repeat unit level. Among all coatings, Poly[NOEGZI-co-NSi] and Poly[NFZI-co-NSi], showed promising results toward nonspecific protein adsorption, with Poly[NFZI-co-NSi] showing the best resistance against most of the proteins tested. Even though both Poly[NC<sub>8</sub>ZI-co-NSi] and Poly[NFZI-co-NSi] were hydrophobic, their affinities toward nonpolar media were quite different. Detailed surface characterization showed that Poly[NFZI-co-NSi] had a lipophobic character, whereas Poly[NC<sub>8</sub>ZI-co-NSi] was lipophilic. This resulted in significant differences in their resistance to protein adsorption, where Poly[NC<sub>8</sub>ZI-co-NSi] showed the highest protein adsorption value. These results suggest that there might be stronger hydrophobic attractions between lipophilic coating components and fouling molecules that are also lipophilic. Therefore, the effectiveness of the Poly[NFZI-co-NSi] in preventing protein adsorption can be attributed to the combination of the zwitterionic functionality with a lipophobic component. The comparison among the fluorinated coatings showed that not only hydrophobic/lipophilic interactions but also the electrostatic attractions should be eliminated to obtain an effective nonfouling material.

## ASSOCIATED CONTENT

### Supporting Information

All experimental procedures, including monomer and polymer synthesis, detailed information about characterization techniques, and additional figures are included. This material is available free of charge via the Internet at <http://pubs.acs.org>.

## AUTHOR INFORMATION

### Notes

The authors declare no competing financial interest.

## ACKNOWLEDGMENTS

This work was supported by Office of Naval Research (N00014-10-1-0348) and National Science Foundation (NSF) (DMR-0805061, DMR-0820506). Mass spectra data were obtained at the University of Massachusetts Mass Spectrometry Facility, which is partially supported by the NSF. Mr. Yongping Zha is greatly acknowledged for his help in obtaining the XRD spectra. We would like to thank Mr. Hitesh Thaker and Mr. Michael Lis for their invaluable comments on early drafts.

## REFERENCES

- (1) Werner, C.; Maitz, M. F.; Sperling, C. J. *Mater. Chem.* **2007**, *17*, 3376–3384.
- (2) Banerjee, I.; Pangule, R. C.; Kane, R. S. *Adv. Mater.* **2011**, *23*, 690–718.
- (3) Kane, R. S.; Deschatelets, P.; Whitesides, G. M. *Langmuir* **2003**, *19*, 2388–2391.
- (4) Hucknall, A.; Rangarajan, S.; Chilkoti, A. *Adv. Mater.* **2009**, *21*, 2441–2446.
- (5) Jiang, S.; Cao, Z. *Adv. Mater.* **2009**, *21*, 1–13.
- (6) Ma, H. W.; Wells, M.; Beebe, T. P.; Chilkoti, A. *Adv. Funct. Mater.* **2006**, *16*, 640–648.
- (7) Ostuni, E.; Chapman, R. G.; Holmlin, R. E.; Takayama, S.; Whitesides, G. M. *Langmuir* **2001**, *17*, 5605–5620.
- (8) Prime, K. L.; Whitesides, G. M. *J. Am. Chem. Soc.* **1993**, *115*, 10714–10721.
- (9) Yang, W.; Xue, H.; Li, W.; Zhang, J.; Jiang, S. *Langmuir* **2009**, *25*, 11911–11916.
- (10) Chen, S.; Jiang, S. *Adv. Mater.* **2008**, *20*, 335–338.
- (11) Holmlin, R. E.; Chen, X. X.; Chapman, R. G.; Takayama, S.; Whitesides, G. M. *Langmuir* **2001**, *17*, 2841–2850.
- (12) Ramsden, J. J. *Chem. Soc. Rev.* **1995**, *24*, 73–78.
- (13) Mrksich, M. A. *Chem. Soc. Rev.* **2000**, *29*, 267–273.
- (14) Cheng, G.; Zhang, Z.; Chen, S.; Bryers, J. D.; Jiang, S. *Biomaterials* **2007**, *28*, 4192–4199.
- (15) Krishnan, S.; Weinman, C. J.; Ober, C. K. *J. Mater. Chem.* **2008**, *18*, 3405–3413.
- (16) Chatelier, R. C.; Xie, X. M.; Gengenbach, T. R.; Griesser, H. J. *Langmuir* **1995**, *11*, 2576–2584.
- (17) Gan, D. J.; Mueller, A.; Wooley, K. L. *J. Polym. Sci., Polym. Chem.* **2003**, *41*, 3531–3540.
- (18) Bartels, J. W.; Cheng, C.; Powell, K. T.; Xu, J.; Wooley, K. L. *Macromol. Chem. Phys.* **2007**, *208*, 1676–1687.
- (19) Gudipati, C. S.; Finlay, J. A.; Callow, J. A.; Callow, M. E.; Wooley, K. L. *Langmuir* **2005**, *21*, 3044–3053.
- (20) Youngblood, J. P.; Andruzzi, L.; Ober, C. K.; Hexemer, A.; Kramer, E. J.; Callow, J. A.; Finlay, J. A.; Callow, M. E. *Proc. Int. Congr. Mar. Corros. Fouling, 11th* **2002**, *11*, 91–98.
- (21) Krishnan, S.; Wang, N.; Ober, C. K.; Finlay, J. A.; Callow, M. E.; Callow, J. A.; Hexemer, A.; Sohn, K. E.; Kramer, E. J.; Fischer, D. A. *Biomacromolecules* **2006**, *7*, 1449–1462.
- (22) Krishnan, S.; Ayothi, R.; Hexemer, A.; Finlay, J. A.; Sohn, K. E.; Perry, R.; Ober, C. K.; Kramer, E. J.; Callow, M. E.; Callow, J. A.; Fischer, D. A. *Langmuir* **2006**, *22*, 5075–5086.
- (23) Martinelli, E.; Menghetti, S.; Galli, G.; Glisenti, A.; Krishnan, S.; Paik, M. Y.; Ober, C. K.; Smilgies, D. M.; Fischer, D. A. *J. Polym. Sci., Polym. Chem.* **2009**, *47*, 267–284.
- (24) Weinman, C. J.; Finlay, J. A.; Park, D.; Paik, M. Y.; Krishnan, S.; Sundaram, H. S.; Dimitriou, M.; Sohn, K. E.; Callow, M. E.; Callow, J. A.; Handlin, D. L.; Willis, C. L.; Kramer, E. J.; Ober, C. K. *Langmuir* **2009**, *25*, 12266–12274.
- (25) Weinman, C. J.; Gunari, N.; Krishnan, S.; Dong, R.; Paik, M. Y.; Sohn, K. E.; Walker, G. C.; Kramer, E. J.; Fischer, D. A.; Ober, C. K. *Soft Matter* **2010**, *6*, 3237–3243.
- (26) Klein, E.; Kerth, P.; Lebeau, L. *Biomaterials* **2008**, *29*, 204–214.
- (27) Hu, K.; Gao, Y.; Zhou, W.; Lian, J.; Li, F.; Chen, Z. *Langmuir* **2009**, *25*, 12404–12407.
- (28) Guo, W.; Tang, X.; Xu, J.; Wang, X.; Chen, Y.; Yu, F.; Pei, M. J. *Polym. Sci., Polym. Chem.* **2011**, *49*, 1528–1534.
- (29) Bartels, J. W.; Billings, P. L.; Ghosh, B.; Urban, M. W.; Greenlief, C. M.; Wooley, K. L. *Langmuir* **2009**, *25*, 9535–9544.
- (30) Cho, Y.; Sundaram, H. S.; Weinman, C. J.; Paik, M. Y.; Dimitriou, M. D.; Finlay, J. A.; Callow, M. E.; Callow, J. A.; Kramer, E. J.; Ober, C. K. *Macromolecules* **2011**, *44*, 4783–4792.
- (31) Shen, M. C.; Martinson, L.; Wagner, M. S.; Castner, D. G.; Ratner, B. D.; Horbett, T. A. *J. Biomater. Sci., Polym. Ed.* **2002**, *13*, 367–390.
- (32) Colak, S.; Tew, G. N. *Langmuir* **2011**, *28*, 666–675.

- (33) Dong, H.; Ye, P.; Zhong, M.; Pietrasik, J.; Drumright, R.; Matyjaszewski, K. *Langmuir* **2010**, *26*, 15567–15573.
- (34) Sambhy, V.; Peterson, B. R.; Sen, A. *Langmuir* **2008**, *24*, 7549–7558.
- (35) Colak, S.; Tew, G. N. *Macromolecules* **2008**, *41*, 8436–8440.
- (36) Colak, S.; Nelson, C. F.; Nusslein, K.; Tew, G. N. *Biomacromolecules* **2009**, *10*, 353–359.
- (37) Erbil, H. Y.; McHale, G.; Rowan, S. M.; Newton, M. I. *Langmuir* **1999**, *15*, 7378–7385.
- (38) Tuteja, A.; Choi, W.; Ma, M.; Mabry, J. M.; Mazzella, S. A.; Rutledge, G. C.; McKinley, G. H.; Cohen, R. E. *Science* **2007**, *318*, 1618–1622.
- (39) Extrand, C. W.; Kumagai, Y. J. *Colloid Interface Sci.* **1997**, *191*, 378–383.
- (40) Honda, K.; Morita, M.; Otsuka, H.; Takahara, A. *Macromolecules* **2005**, *38*, 5699–5705.
- (41) Corpart, J. M.; Girault, S.; Juhue, D. *Langmuir* **2001**, *17*, 7237–7244.
- (42) Honda, K.; Morita, M.; Sakata, O.; Sasaki, S.; Takahara, A. *Macromolecules* **2010**, *43*, 454–460.
- (43) Wang, Q.; Zhang, Q.; Zhan, X.; Chen, F. J. *Polym. Sci., Polym. Chem.* **2010**, *48*, 2584–2593.
- (44) Owens, D. K.; Wendt, R. C. J. *Appl. Polym. Sci.* **1969**, *13*, 1741–1747.
- (45) Hu, Z.; Finlay, J. A.; Chen, L.; Betts, D. E.; Hillmyer, M. A.; Callow, M. E.; Callow, J. A.; DeSimone, J. M. *Macromolecules* **2009**, *42*, 6999–7007.
- (46) Gudipati, C. S.; Greenlief, C. M.; Johnson, J. A.; Prayongpan, P.; Wooley, K. L. *J. Polym. Sci., Polym. Chem.* **2004**, *42*, 6193–6208.
- (47) Gudipati, C. S.; Greenlief, C. M.; Johnson, J. A.; Prayongpan, P.; Wooley, K. L. *Langmuir* **2005**, *21*, 3044–3053.
- (48) Ozeki, K.; Nagashima, I.; Hirakuri, K. K.; Masuzawa, T. *J. Mater. Sci.: Mater. Med.* **2010**, *21*, 1641–1648.
- (49) Balasubramanian, V.; Slack, S. M. J. *Biomater. Sci., Polym. Ed.* **2002**, *13*, 543–561.
- (50) Balasubramanian, V.; Grusin, N. K.; Bucher, R. W.; Turitto, V. T.; Slack, S. M. J. *Biomed. Mater. Res.* **1999**, *44*, 253–260.
- (51) Voros, J. *Biophys. J.* **2004**, *87*, 553–561.
- (52) Jeon, S. I.; Andrade, J. D. J. *Colloid Interface Sci.* **1991**, *142*, 159–166.
- (53) Malmsten, M. *Abstr. Pap. Am. Chem. Soc.* **1994**, *207*, 71-COLL.
- (54) Defejter, J. A.; Benjamins, J.; Veer, F. A. *Biopolymers* **1978**, *17*, 1759–1772.
- (55) Elwing, H. *Biomaterials* **1998**, *19*, 397–406.
- (56) Kim, J.; Somorjai, G. A. *J. Am. Chem. Soc.* **2003**, *125*, 3150–3158.
- (57) Togashi, D. M.; Ryder, A. G.; Heiss, G. *Colloids Surf., B* **2009**, *72*, 219–229.
- (58) Tsai, W. B.; Grunkemeier, J. M.; Horbett, T. A. *J. Biomed. Mater. Res.* **1999**, *44*, 130–139.
- (59) Herrwerth, S.; Eck, W.; Reinhardt, S.; Grunze, M. *J. Am. Chem. Soc.* **2003**, *125*, 9359–9366.
- (60) Kong, C. F.; Fung, B. M.; Orear, E. A. *J. Phys. Chem.* **1985**, *89*, 4386–4390.
- (61) Held, P.; Lach, F.; Lebeau, L.; Mioskowski, C. *Tetrahedron Lett.* **1997**, *38*, 1937–1940.
- (62) Mukerjee, P.; Handa, T. *J. Phys. Chem.* **1981**, *85*, 2298–2303.